oceans

MDPI

Article

Effects of Natural and Artificial Surfactants on Diffusive Boundary Dynamics and Oxygen Exchanges across the Air–Water Interface

Adenike Adenaya [1,*], Michaela Haack [1,2], Christian Stolle [1,3,4], Oliver Wurl [1] and Mariana Ribas-Ribas [1]

[1] Center for Marine Sensors, Institute for Chemistry and Biology of the Marine Environment, Carl von Ossietzky Universität Oldenburg, 26382 Wilhelmshaven, Germany; michaela.c.haack@gmail.com (M.H.); christian.stolle2@uni-oldenburg.de (C.S.); oliver.wurl@uni-oldenburg.de (O.W.); mariana.ribas.ribas@uni-oldenburg.de (M.R.-R.)
[2] KRÜSS GmbH, 22453 Hamburg, Germany
[3] Leibniz Institute for Baltic Sea Research, 18119 Rostock, Germany
[4] Project Management Jülich, 18069 Rostock, Germany
* Correspondence: adenike.adenaya@uni-oldenburg.de

Abstract: Comparing measurements of the natural sea surface microlayer (SML) and artificial surface films made of Triton-X-100 and oleyl alcohol can provide a fundamental understanding of diffusive gas fluxes across the air–water boundary layers less than 1 mm thick. We investigated the impacts of artificial films on the concentration gradients and diffusion of oxygen (O_2) across the SML, the thickness of the diffusive boundary layer (DBL), and the surface tension levels of natural seawater and deionized water. Natural and artificial films led to approximately 78 and 81% reductions in O_2 concentration across the surfaces of natural seawater and deionized water, respectively. The thicknesses of the DBL were 500 and 350 µm when natural SML was added on filtered and unfiltered natural seawater, respectively, although the DBL on filtered seawater was unstable, as indicated by decreasing thickness over time. Triton-X-100 and oleyl alcohol at a concentration of 2000 µg L^{-1} in deionized water persistently increased the DBL thickness values by 30 and 26% over a period of 120 min. At the same concentration, Triton-X-100 and oleyl alcohol decreased the surface tension of deionized water from ~72 mN m^{-1} to 48 and 38 mN m^{-1}, respectively; 47% recovery was recorded after 30 min with Triton-X-100, although low surface tension persisted for 120 min with oleyl alcohol. The critical micelle concentration values of Triton-X-100 ranged between 400 and 459 µg L^{-1}. We, therefore, suggest that Triton-X-100 resembles natural SML because the reduction and partial recovery of the surface tension of deionized water with the surfactant resembles the behavior observed for natural slicks. Temperature and salinity were observed to linearly decrease the surface tension levels of natural seawater, artificial seawater, and deionized water. Although several factors leading to O_2 production and consumption in situ are excluded, experiments carried out under laboratory-controlled conditions are useful for visualizing fine-scale processes of O_2 transfer from water bodies through the surface microlayer.

Keywords: oxygen outflux; diffusive boundary layer; surface tension; surfactants; sea surface microlayers

Citation: Adenaya, A.; Haack, M.; Stolle, C.; Wurl, O.; Ribas-Ribas, M. Effects of Natural and Artificial Surfactants on Diffusive Boundary Dynamics and Oxygen Exchanges across the Air–Water Interface. *Oceans* **2021**, *2*, 752–771. https://doi.org/10.3390/oceans2040043

Academic Editors: Michael W. Lomas and Antonio Bode

Received: 31 January 2021
Accepted: 15 November 2021
Published: 24 November 2021

1. Introduction

The impacts of surfactants on natural seawater cannot be overemphasized, as most surfactants are known to accumulate at the interface between the ocean and the atmosphere. This interface is ubiquitous and generally known as the sea surface microlayer (SML). It represents the uppermost part of the ocean that is always in contact with the atmosphere [1]. The SML connects the ocean to the atmosphere and controls many physical, chemical, and biological processes in the global ecosystem and climate physics [2,3], with the most prominent of the latter being the exchange of gases between the ocean and the atmosphere [3]. Air–water gas fluxes depend on near-surface turbulence generated by wind

forcing [4], small-scale waves [5], microbreaking [6], while the availability of surface active agents, i.e., biogenic surfactants, modify these by forming a thin laminar SML. Recently, Mustaffa et al. [3] showed that natural SMLs reduce the air–water transfer velocity (k) by up to 63%.

The commonly studied mechanisms of gaseous flux through the ocean boundary are molecular and turbulent transport [1,2]. Although estimates of the two transport mechanisms remain uncertain, many studies have suggested that the mass gaseous transfer through the SML is mediated by molecular diffusion [7]. This mechanism, however, is largely dependent on the solubility and molecular diffusivity of the transported gas, as well as the thickness of the diffusive boundary layer (DBL) of seawater. When gas is transferred from the air to the water or vice versa, it passes through the diffusion layers by molecular diffusion [8]. The DBL forms a thin film measuring less than 1 mm on the water surface and reduces the diffusion rates of many dissolved entities [9]. This, in turn, influences the exchange of oxygen and other gases across marine interfaces [8,9]. The oxygen concentration in the DBL is solely controlled by its gross production and subsequent consumption through photosynthetic and respiratory activities of planktonic cells [10,11].

By investigating the vertical and temporal variability of the oxygen gradient across the SML, Rahlff et al. [11] showed that the concentration gradient of oxygen across the SML over stagnant water bodies was driven by its diffusion in or out of bulk water. They also showed that the oxygen concentration in stagnant water was produced or consumed by planktonic activities but not by the microbes inhabiting the SML, the so-called neuston. The diffusion of oxygen between the ocean and the atmosphere is determined by its partial pressure and its gradient across the SML [12].

The SML and its enrichment by surfactants can impede gaseous flux across the interface, depending on the molecular properties of the surfactant and the thickness of the SML [3]. Surfactants can be grouped into four concentration regimes that occur in natural seawater according to their reduction levels of gas fluxes [3,13]. The low and medium surfactant regimes ranges are 50–200 and 200–400 μg L^{-1}, respectively. The high surfactant regime range is 400–650 μg L^{-1} [3], while surfactants with concentrations of 800 μg L^{-1} and above are observed in natural slicks [14]. Surfactants exert wave-damping effects on ocean surfaces, even at low concentrations (50–300 μg L^{-1}) [15,16], and are also known to form micelles in bulk water.

The formation of micelles by surfactants occurs when the surfactant molecules at a particular concentration can no longer accumulate in the monolayer at the surface [16]. Since surfactants prefer to adsorb to liquid surfaces, they lower the surface tension of the liquid [17]. Molecularly, the force of attraction between the molecules in the bulk liquid is balanced; they are in a favorable energetic state compared to molecules on the surface of the liquid, because the latter lack neighboring molecules, causing unbalanced forces. Theoretically, they are pulled into the bulk liquid. This is avoided by the formation of a strong intermolecular (cohesive) force, which results in tension being created on the surface [17].

The surface tension of a liquid decreases to a large extent with increasing temperature, salinity, and surfactant [18]. For instance, Schmidt and Schneider [19] observed a linear relationship between these three factors and measured the surface tension of deionized water and natural seawater at a temperature range of 5 to 35 °C using the Wilhelmy plate method. They observed that the surface tension decreased with increased temperature.

Microsensors have been used for several years to investigate oxygen concentration and consumption in marine sediments [12], to monitor the rate of respiration in benthic environments [20], and more recently to evaluate oxygen concentration gradients across the SML [11]. A study on temporal changes in oxygen concentrations in seawater in Jade Bay by Rahlff et al. [11] revealed increased oxygen concentrations from the air–water interface (i.e., infinite top layer) to a depth of about 1 mm and a subsequent decrease mediated mostly by biological activities. They concluded that the metabolic impact of the neuston on

oxygen concentrations in the SML was negligible compared to the influence of plankton metabolic activity.

This study aims to understand oxygen transfer in the presence of surface films and their varying compositions at a more mechanistic level. Using Clark-type microsensors, we estimated the impacts of SML and artificial surface films (Triton-X-100 and oleyl alcohol) on oxygen diffusion rates across the surface of natural seawater and deionized water. In addition, the thicknesses of DBLs in seawater and deionized water samples and their influence on the diffusive flux of O_2 across a stagnant water surface were examined with the addition of natural SMLs and artificial surfactants, respectively. Lastly, we focused on the surface tension of the SML in comparison to artificial surface films. We used the Wilhelmy method to evaluate and compare the correlations between the surface tension levels of the SML, deionized water, and artificial seawater.

2. Materials and Methods

2.1. Sample Collection

SML and natural seawater samples were collected from Jade Bay between November 2017 and November 2019. Jade Bay (53°28′42″ N 8°12′15″ E) a tidal bay located in the North Sea, which links to the Wadden Sea through outer Jade Bay, located in the western part of Wilhelmshaven [21]. SML samples were collected using the glass plate method first described by Harvey and Burzell [22]. A glass plate (30 × 40 cm) was immersed vertically into the underlying water and then withdrawn at a rate of approximately 5 cm per second to allow the SML to adhere to the plate based on capillary forces. The attached SML sample was then transferred into a sterile brown bottle from the glass plate with a squeegee. The process was repeated until the required volume (100 mL) was obtained. The glass plate was cleaned with 70% ethanol prior sampling.

To investigate seasonal effects on O_2 concentration and diffusion across the interface, three natural seawater samples were collected, in November 2017 (autumn), January 2018 (winter), and July 2018 (summer). The sampling dates, sample types and periods of sampling are summarized in Table 1. Seawater samples were collected from a depth of 1 m using a syringe connected to a hose. A portion of the samples was filtered through 3.0 and 0.2 µm membrane filters (polycarbonate; Sartorius, Sartorius, Göttingen, Germany) to remove surface active particles. A portion of the natural seawater samples used for surface tension and temperature measurements was filtered through 0.2 µm membrane filters.

Table 1. Sample collection dates and periods.

Sample Dates	Samples	Periods
6 November 2017	Unfiltered natural	
7 November 2017	seawater	Autumn
7 November 2017		
6 November 2017	Unfiltered natural	Autumn
22 January 2018	seawater and	Winter
6 July 2018	unfiltered SML	Summer
24 January 2018	Filtered natural	Winter
31 January 2018	seawater	Winter
5 July 2018		Summer
24 January 2018	Filtered natural seawater	Winter
5 July 2018	And filtered SML	Summer
5 November 2018		Autumn
November 2018	Deionized water	-
November 2018	Triton-X-100	-
November 2018	oleyl alcohol	-
November 2019	Natural seawater	-
November 2019	Artificial seawater	-

Artificial seawater was prepared using Trophic Marin Reef Mix (Trophic Marin, Wartenberg, Germany), and deionized water was generated through a laboratory-based ultrapure water system (Sartorius, Göttingen, Germany). The artificial seawater was diluted 1:1 and 1:4 with deionized water, and the salinity of each dilution (Table 2) was measured using a conductivity sensor (CyberScan PCD 650; Oakton Instruments, Vernon Hills, IL, USA).

Table 2. Measured salinity of artificial seawater.

Artificial Seawater	Temperature (°C)	Salinity
No dilution	20.7	39.7
1:1	20.7	23.2
1:4	20.7	9.9

2.2. Measurement of O_2 Concentration and Diffusive Boundary Layer (DBL) in Natural Seawater and Deionized Water

We investigated the effects of surface films (SML and artificial surfactants) on O_2 diffusion across the SML and artificial films on top of natural seawater and deionized water samples, respectively, with Clark-type OX-50 and TP-200 microsensors (Unisense, Aarhus, Denmark). Both sensors were connected to a picoammeter (Unisense Microsensor Multimeter, Denmark). The OX-50 sensor was calibrated using 100% O_2 saturated water and 0% O_2 saturated (anoxic) sodium ascorbate solution (0.1 M). The response times of the sensors were <5 and <3 s, respectively. O_2 concentrations and diffusion rates across the SML and artificial films were calculated from O_2 gradients using a micro-profiling system controlled by the Unisense SensorTraceSuite software package (version 2.6.100, Unisense, Aarhus, Denmark). Both sensors were fixed to a micromanipulator stage, which in turn was attached to a motor stage that performed microscale movements. The microscale movements were controlled by using the profiling settings in the Unisense software package (Unisense, Aarhus, Denmark). The sensors were inserted upside down into a 4 L water sample (beaker was approximately 227 mm in diameter) with their tips positioned about 3000 µm below the water surface (Figure 1). We moved the electrode from the bottom upward to reduce any interference on the laminar layer by the actual movement. The motor was programmed so that every 3 s it moved the electrodes 100 µm upward, allowing it to record dissolved O_2 concentrations and temperature gradients toward and across the water surface.

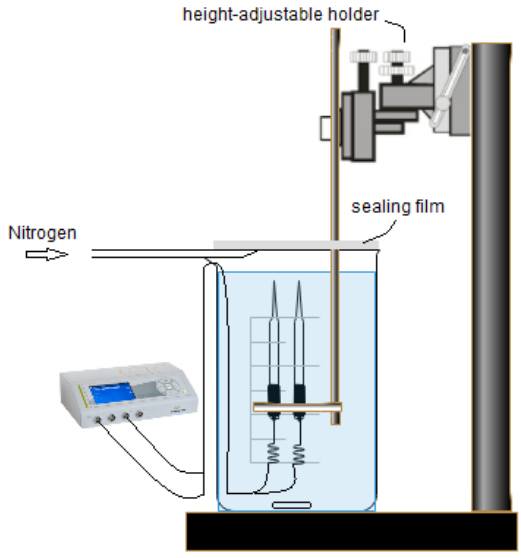

Figure 1. OX-50 and TP-200 microsensors were inserted upside down into 4 L water samples with their tips positioned about 3000 µm below the water surface to measure O_2 and temperature gradients across SML and artificial surface films.

The exchange of O_2 was computed from O_2 gradients measured directly from natural seawater samples (filtered and unfiltered) without SML and samples (filtered and unfiltered) with 22.7 mL of SML samples (filtered and unfiltered). This SML volume corresponded to a thickness of 1.1 mm in the beaker, which is representative of the thickness of biofilm-like slicks [23]. Slicks are visible on the sea surface and are caused by reduced surface roughness due to the high enrichment of organic matter. It has been estimated that slicks cover 10% of the open ocean [24] and reduce the CO_2 air–sea gas velocity by 60% [3].To force a net flux of oxygen into the overlying air, an artificial gradient of dissolved O_2 was created by covering the beakers containing seawater and deionized water samples with parafilm and then creating an O_2-free headspace over the water with a constant 0.1 bar of nitrogen gas [19]. With a N_2 atmosphere, the readings of the oxygen sensors indicated when the sensor tip left the aqueous phase. This procedure was also intended to keep the sensor tips in position while measuring and to allow for easy reproducibility of the experiment. In this way, the O_2 concentration was measured from the air–water interface of each profile. The O_2 concentrations of the profiles and their equivalent signal values were temperature-corrected and converted into μmol O_2 L^{-1} min^{-1}, as previously described by Rahlff et al. [11]. The mean O_2 concentration was then deduced every 60 min in each case and the average diffusion within 2 h was calculated using the Whitman film model described by Rahlff et al. [11]. In addition, as it was previously estimated by Rahlff et al. [11] that a significant amount of O_2 is consumed biologically, the biological activities leading to O_2 consumption in natural seawater samples were assessed by comparing the O_2 concentrations in filtered and unfiltered samples. Samples were not changed for every profile. The measurements were taken in triplicate and the mean as well as the standard deviation were calculated.

The impacts of surfactants and their effect on thickening the DBL and reducing gas exchange across the water–air interface were examined by adding 2000 μg L^{-1} each of Triton-X-100 and oleyl alcohol to the surfaces of the deionized water samples. We used these two surfactants because oleyl alcohol is well known as a reference material in film studies related to air–water gas exchange [9] due to its formation of monolayers, while Triton-X-100 is the standard compound used to calibrate bulk measurements of marine surfactants [22]. While oleyl alcohol forms monolayers with a high spread rate and film stability, Triton-X-100 has a hydrophilic chain and hydrophobic aromatic ring, and in contrast, mixes with water but still retains its surface-active properties. As a result, it has been used to quantify complex mixtures of surface-active compounds as Triton-X-100 equivalent (Teq) in the marine environment, including the SML [22,23]. Concentrations ranging from 13 to 2000 μg L^{-1} of each artificial surfactant were also used to investigate changes in DBL thickness.

A magnetic stirrer moving at 250 rpm was used to gently stir the liquid during the measurements. We then calculated DBL values in μm from the O_2 concentration gradients by fitting three lines into the data obtained from temperature-corrected gradients. Two of the lines were the constant oxygen concentration in the air and the bulk water, and the third line was fitted on the surface, where the change in oxygen concentration started from the depth, i.e., the sensor tip penetrated through the water surface. The DBL was then calculated from the difference between the depths where the surface line crossed the two constant lines.

This approach was also applied to filtered and unfiltered natural seawater to assess the effects of biological activities. We evaluated the DBL thicknesses of these samples with and without SML for comparison and to estimate their role in creating a barrier layer. To understand the dynamics of DBL thickness and surface film concentrations, we conducted measurements with natural seawater and deionized water with and without SML and artificial surfactants, respectively.

2.3. Surface Tension Measurements

2.3.1. Surface Tension as a Function of Temperature and Salinity

The K100 force tensiometer (Krüss, Germany) used for the measurement of surface tension uses a force sensor that measures the force exerted on a roughened platinum plate. The temperature of the samples is controlled through a water bath with a connected temperature sensor. The surface tension values of all samples were recorded using the software package (version 1.10-01, Krüss, Hamburg, Germany). The platinum plate (PL01/PLC01), with a wetted length of 40.2 mm, was flamed and carefully hung on the force sensor. The washed and dried sample vessel (SV 20), with a diameter of 70 mm, was filled with 34.7 mL of liquid sample (deionized water, natural and artificial seawater, or SML) and placed on the sample stage. It was then raised up to the force sensor by using the control pad of the force tensiometer until the plate was very close to the surface of the liquid. The plate was in contact with the surface of the liquid and pulled up slowly, and the force acting on the sensor when the plate touched the surface was measured. This was then used to deduce the surface tension of the samples. Each sample was analyzed in triplicate and the mean and standard deviation were calculated.

2.3.2. Surface Tension of Deionized Water with Triton-X-100 and Oleyl Alcohol

We analyzed the impact of artificial surfactants on the surface tension of water with three different experiments. In the first experiment, we investigated the effects of different concentrations of Triton-X-100 (Carl Roth, Karlsruhe, Germany) on the surface tension and formation of micelles in the bulk deionized water sample. Different volumes of surfactant were added to a constant total volume of 37.4 mL deionized water. The surface tension of the water sample was measured with increasing surfactant concentrations. Measurements were taken in triplicate and the mean and standard deviation were calculated. In the second experiment, the dynamic and time-dependent effects of films made by Triton-X-100 and oleyl alcohol on the surface tension of deionized water samples were investigated. For this, 2000 $\mu g\ L^{-1}$ of each surfactant was gently laid onto deionized water in a 2.5 L beaker with 226.98 cm^2 surface area. Measurements were taken every 30 min, for a total duration of 120 min. Each measurement was carried out in triplicate (pseudo-replicates). In the third experiment, the degree of recovery of the surface tension of deionized water was analyzed after the addition of different concentrations of Triton-X-100 and oleyl alcohol ranging from 13 to 2000 $\mu g\ L^{-1}$, representing concentrations in natural SMLs. Triplicate measurements were carried out within 10 min. To ensure homogeneous distribution of surfactants in the deionized bulk water phase, a stirrer was used to stir the solution thoroughly before measurements.

3. Results

3.1. O_2 Concentration Loss Diffusive Outflux in Natural Seawater and Deionized Water

We observed temporal and spatial variations in O_2 concentrations, although there was a decreasing trend of concentration after 120 min (Figure 2a–f). Table 3 summarizes the O_2 concentrations and outflux rates obtained at each time point for our filtered and unfiltered seawater samples obtained in autumn, winter, and summer, as well as the deviations between replicated measurements. There were also variations in sample temperatures, as the highest temperatures were measured in summer samples.

We calculated the average O_2 diffusion rate from the slopes of O_2 concentration gradients with their respective time periods in all seawater samples (filtered and unfiltered) and observed that all rates were negative and ranged from -0.47 µmol to -0.02 µmol L^{-1} min^{-1} (Table 3). The loss in O_2 concentration over time in filtered natural seawater was higher, with a 16% loss of oxygen within 120 min compared to a 10% loss in unfiltered natural seawater. Interestingly, the addition of SML almost halted the exchange of O_2 from the water to the nitrogen phase over a period of at least 2 h (Table 3). For example, filtered seawater collected in winter lost ~16% or 18.7 µmol L^{-1} of its total concentration in 60 min, but when the same sample was covered with natural SML, the loss was reduced to 1.7%

or 1.6 µmol L^{-1} in 60 min. The same trend was observed for unfiltered and filtered seawater samples obtained in autumn and summer. The addition of SML on the surfaces of unfiltered and filtered seawater suppressed O_2 exchange by 44 and 66%, respectively.

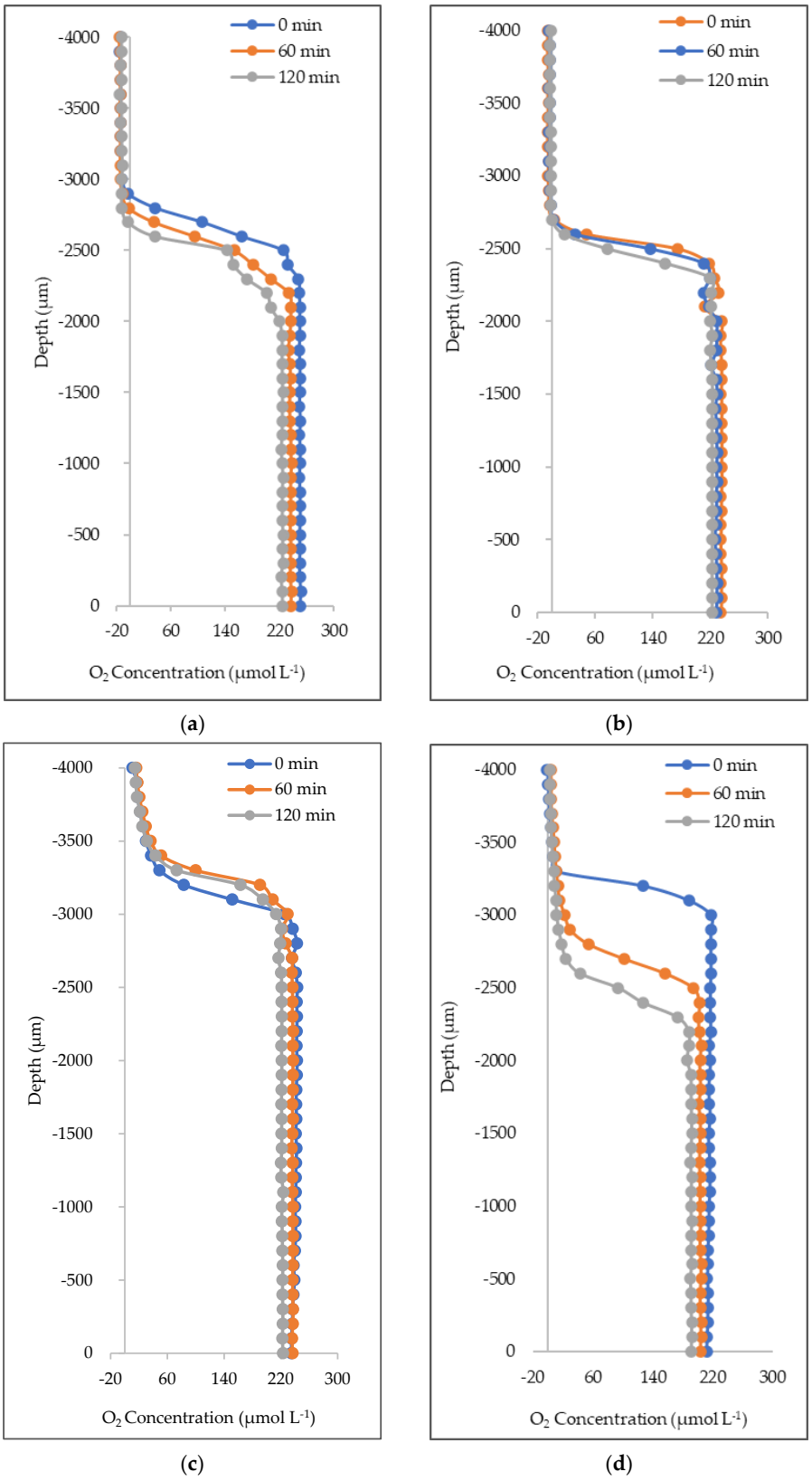

Figure 2. *Cont.*

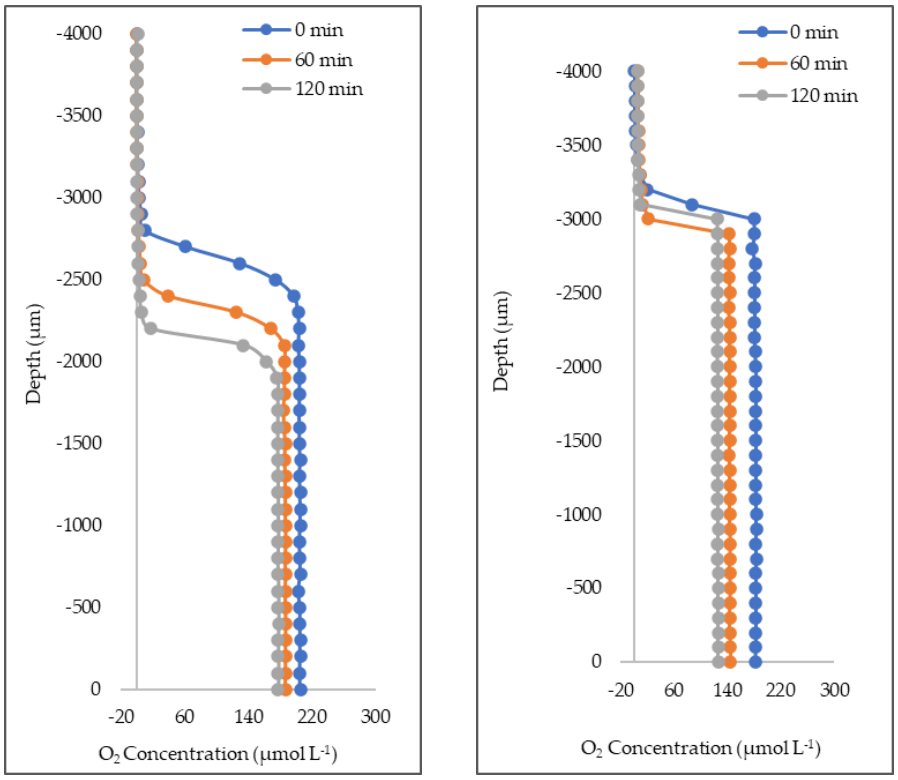

Figure 2. Example profiles of oxygen concentrations in (**a**) unfiltered seawater, autumn; (**b**) unfiltered seawater + SML, autumn; (**c**) unfiltered seawater + SML, winter; (**d**) filtered seawater, winter; (**e**) unfiltered seawater + SML, summer; (**f**) filtered seawater, summer.

Table 3. Spatial and temporal variations of O_2 concentration, outflux rate, and temperature in natural seawater samples collected in autumn, winter, and summer. Each temperature-corrected O_2 concentration (µmol L^{-1}) was obtained from the temperature, intercept, and slope of each sensor signal after applying linear regression to all treatments. Errors are based on standard deviations (n = 3) between pseudo-replicated measurements.

Time (min)	Autumn Unfiltered (µmol L^{-1})	Autumn Unfiltered + SML (µmol L^{-1})	Winter Unfiltered + SML (µmol L^{-1})	Winter Filtered (µmol L^{-1})	Winter Filtered + SML (µmol L^{-1})	Summer Unfiltered + SML (µmol L^{-1})	Summer Filtered (µmol L^{-1})	Summer Filtered+ SML. (µmol L^{-1})
0	250.1 ± 3	235.2 ± 5	239.0 ± 3	234.6 ± 28	186.9 ± 2	205.6 ± 1	182.8 ± 0	211.1 ± 70
60	237.8 ± 2	228.8 ± 1	236.6 ± 1	217.9 ± 19	182.9 ± 1	187.6 ± 0	146.9 ± 0	201.2 ± 72
120	226.3 ± 3	222.5 ± 0	222.1 ± 1	197.3 ± 8	183.8 ± 2	177.8 ± 0	126.0 ± 0	188.8 ± 72
Loss per hour	11.9 ± 0	6.4 ± 5	8.5 ± 2	18.7 ± 20	1.6 ± 0	13.9 ± 1	28.4 ± 0	11.2 ± 1
% loss	9.6	5.4	7.1	15.9	1.7	13.6	31.1	10.6
				O_2 Outflux (µmol O_2 L^{-1} min^{-1})				
t_0-t_{120}	−0.19	−0.10	−0.14	−0.31	−0.02	−0.23	−0.47	−0.19
				Temperature (°C)				
0	13.6 ± 2	13.1 ± 0	9.8 ± 0	13.4 ± 3	15.9 ± 1	17.3 ± 1	17.9 ± 0	17.2 ± 0
60	15.09 ± 1	14.7 ± 0	11.7 ± 0	14.4± 0	15.9 ± 1	16.6 ± 0	17.6 ± 0	17.1 ± 0
120	15.8 ± 1	16.1 ± 0	13.0 ± 0	15.2 ± 2	15.9 ± 0	16.4± 0	17.6 ± 0	17.3 ± 0

To simulate oxygen outgassing crossing surfactant films, we covered the surfaces of deionized water separately with 2000 µg L^{-1} of Triton-X-100 and oleyl alcohol and left uncovered deionized water, i.e., without artificial surfactants, as the control. The O_2 concentrations from the top 0 to 200 µm surface of the sample with and without artificial surfactant were calculated from the gradient (data stored in PANGAEA: https://doi.org/10.1594/PANGAEA.937780 (accessed on 10 November 2021), and the mean values are given in Table 4. The rate at which O_2 diffused from the control water sample

was also observed to be higher compared to the deionized water with artificial surfactants. Approximately 17% of the measured dissolved O_2 concentration was lost from deionized water samples without treatment in 60 min. The addition of 2000 μg L^{-1} of artificial surfactants (Triton-X-100 or oleyl alcohol) on the surface had a severe impact on the oxygen exchange. Triton-X-100 inhibited oxygen transfer by ~64%, while oleyl alcohol reduced transfer by 98%. The average diffusive rate for the samples without surfactant was −0.32 μmol L^{-1} min^{-1}, while those of the samples containing Triton-X-100 and oleyl alcohol were −0.20 and −0.009 μmol L^{-1} min^{-1}, respectively.

Table 4. O_2 concentrations in deionized water samples with and without artificial surfactant and their respective temperatures. Errors are based on average standard deviations obtained from variations between 3 replicates (n = 3) for each treatment.

Time (min)	Deionized Water (μmol L^{-1})	Deionized Water + Triton-X-100 (μmol L^{-1})	Deionized Water + Oleyl Alcohol (μmol L^{-1})
0	237.3 ± 4	253.3 ± 40	241.8 ± 6
60	215.8 ± 8	243.9 ± 32	251.0 ± 7
120	198.2 ± 7	228.9 ± 17	240.8 ± 8
loss per hour	19.4 ± 3	12.2 ± 23	0.5 ± 0
% loss	16.5	9.6	0.4
		O_2 outflux (μmol O_2 L^{-1} min^{-1})	
t_0-t_{120}	−0.32	−0.20	−0.009
		Temperature (°C)	
0	21.1 ± 1	19.1 ± 1	19.6 ± 2
60	20.0 ± 1	18.4 ± 1	20.0 ± 2
120	19.6 ± 2	19.1 ± 2	20.8 ± 2

3.2. Thickness of Diffusive Boundary Layer (DBL)

Without artificial surfactants, DBL measurements in deionized water samples revealed a thickness of 319 ± 28 μm, which increased to 352 ± 28 μm over a period of 120 min. Meanwhile, there was no significant difference in observed thickness with 2000 μg L^{-1} of oleyl alcohol over a period of at least 120 min. The same concentration of Triton-X-100, however, caused an initial thickness of 473 ± 6 μm, which increased to 550 ± 5 μm within 120 min (Table 5). For all time points, the mean DBL thickness in deionized water without treatment was calculated to be 321 ± 41 μm, while those in deionized water treated with Triton-X-100 or oleyl alcohol were 493 ± 14 and 442 ± 27 μm, respectively (Figure 3a).

Table 5. DBL thicknesses obtained from deionized water with and without artificial surfactant (2000 μg L^{-1} each of oleyl alcohol and Triton-X-100). Each DBL was given by the intercept, slope of depth, and temperature-corrected O_2 concentration after applying linear regression to all treatments. Standard deviations (n = 3) were calculated for each time point.

	Diffusive Boundary Layers		
Time (min)	Deionized Water (μm)	Deionized Water + Oleyl Alcohol (μm)	Deionized Water + Triton-X-100 (μm)
30	319 ± 28	423 ± 10	473 ± 6
60	294 ± 16	481 ± 72	457 ± 29
120	352 ± 28	424 ± 8	550 ± 5

Figure 3b shows the mean DBL thicknesses for all seawater samples. As expected, unfiltered natural seawater was found to form a thicker DBL (mean 404 ± 59 μm) compared to filtered water (mean 364 μm ± 49 μm). The addition of natural SML on the surfaces of these samples strongly influenced DBL thickness in different ways. The addition of SML increased the thickness in filtered natural seawater from 416 ± 53 to 499 ± 49 μm within 30 min of measurement. This increment was not persistent with time, as the DBL decreased to 412 ± 13 μm after 120 min.

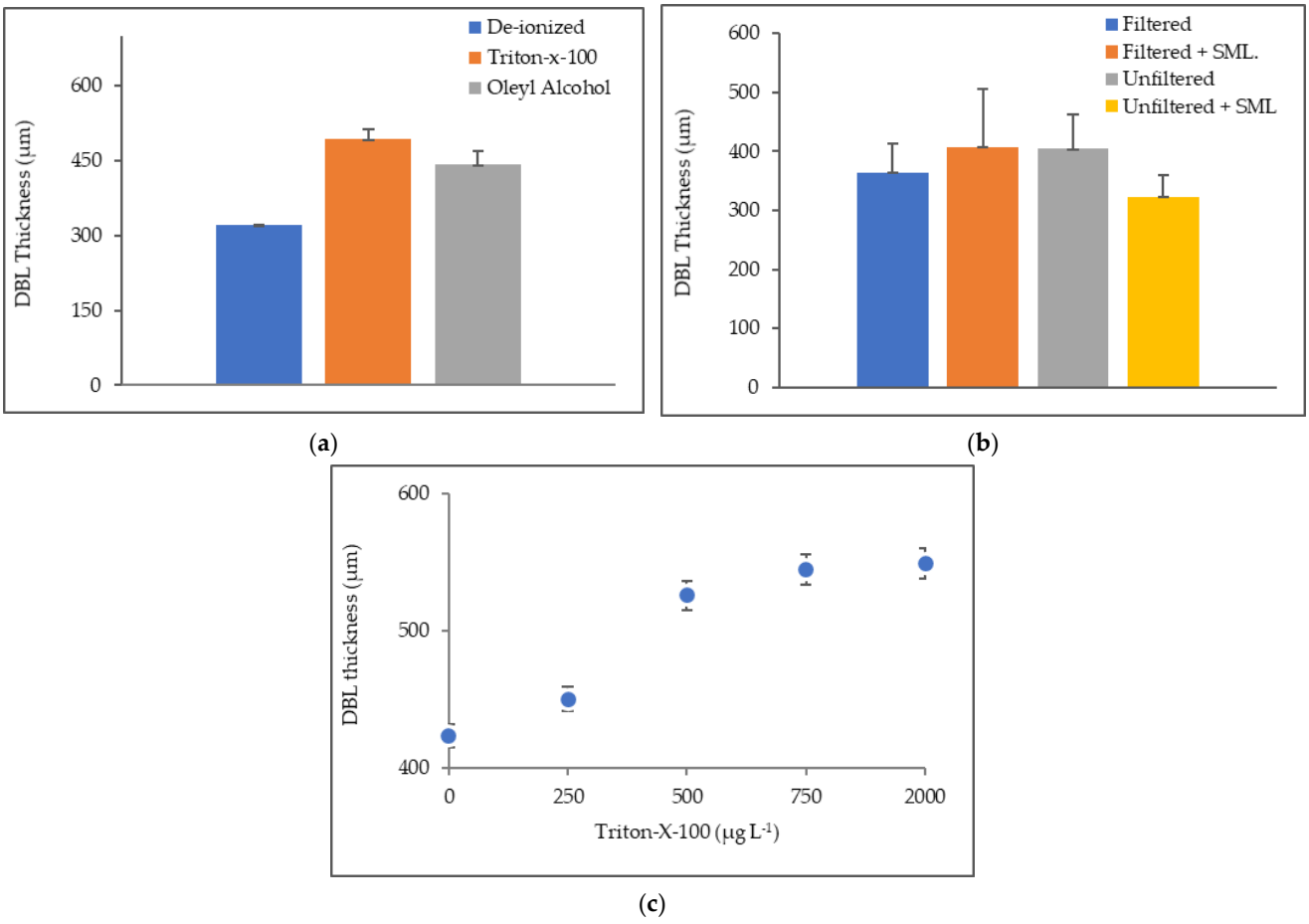

Figure 3. (**a**) Mean DBL thicknesses in deionized water with and without artificial surfactant (2000 µg L^{-1} each of oleyl alcohol and Triton-X-100). Artificial surfactant caused an apparent increase in DBL of deionized water. (**b**) Mean DBL thicknesses in filtered and unfiltered natural seawater with and without SML. Values were obtained from the slope and intercept of O_2 concentration between air and bulk water and their respective depths. (**c**) Different concentrations of Triton-X-100 linearly increased DBL thickness.

On the contrary, the high DBL thickness observed in unfiltered seawater of 459 ± 24 µm was unexpectedly reduced to 333 ± 45 µm 30 min after the addition of unfiltered SML. This decrease in DBL thickness was observed to continue to 283 ± 58 µm after 120 min, i.e., at the end of our time series (Table 6). Comparing DBL thicknesses from time point t_{30} to t_{120}, we observed that the thickness decreased by 98 ± 47 µm in filtered seawater and increased by 35 ± 9 µm in unfiltered seawater.

Table 6. DBL thicknesses calculated for filtered and unfiltered natural seawater (with and without SML). DBL thickness values were obtained from the intercept and slope of O_2 profile measurements and the mean of all replicated measurements was calculated. The standard deviation (n = 3) was calculated for each time point. A linear regression line was applied to the depth- and temperature-corrected O_2 concentration.

Diffusive Boundary Layers				
Time (min)	**Filtered (µm)**	**Filtered + SML. (µm)**	**Unfiltered (µm)**	**Unfiltered + SML (µm)**
30	416 ± 53	499 ± 49	348 ± 41	351 ± 41
60	357 ± 54	303 ± 31	459 ± 24	333 ± 45
120	318 ± 6	412 ± 13	383 ± 32	283 ± 58

When we examined the impacts of various concentrations of Triton-X-100 on DBL thicknesses in deionized water samples, it was observed that the thickness increased from 423 ± 37 to 525 ± 13 µm when 500 µg L^{-1} of Triton-X-100 was added. A further slight increase to 545 ± 22 µm was observed with a concentration of 750 µg L^{-1}, and then the value remained constant with a concentration of 2000 µg L^{-1} of Triton-X-100 (Figure 3c).

3.3. Surface Tension as a Function of Temperature and Salinity

The average surface tension obtained for deionized water at 24 ± 1 °C was 71.82 ± 2 mN m^{-1}, which decreased to 64.03 ± 2 mN m^{-1} at 55 ± 1 °C. The surface tension values of unfiltered and filtered natural seawater at 24 ± 2 °C were 70.94 ± 1 and 70.50 ± 1 mN m^{-1}, respectively (Figure 4a). Natural filtered and unfiltered seawater showed similar relationships with temperature, as they decreased to 64.08 ± 2 and 66.68 ± 2 mN m^{-1}, respectively, at 55 ± 1 °C (Figure 4b). The artificial seawater sample, with a salinity of 39.7, had a surface tension of 71.73 ± 1 mN m^{-1}, while the artificial seawater samples, with salinity levels of 23.2 and 10.0, had surface tension values of 70.67 ± 1 and 69.53 ± 1 mN m^{-1}, respectively, at 25 ± 1 °C. The surface tension levels of the three artificial seawater categories decreased linearly to 67.87 ± 2, 66.86 ± 3, and 66.40 ± 2 mN m^{-1}, respectively, at 51 ± 3 °C. The linear relationship was disrupted, as the surface tension levels of the three types of artificial seawater samples decreased sharply to 57.18 ± 4, 55.10 ± 6, and 61.40 ± 7 mN m^{-1}, respectively, at 55 ± 1 °C (Figure 4c).

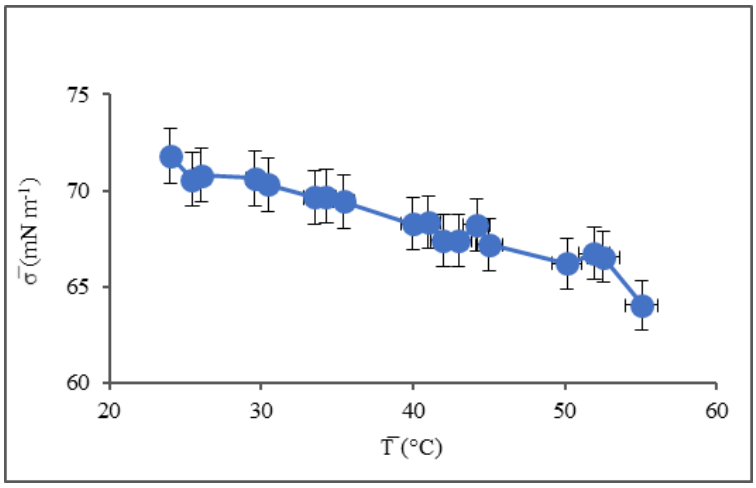

(**a**)

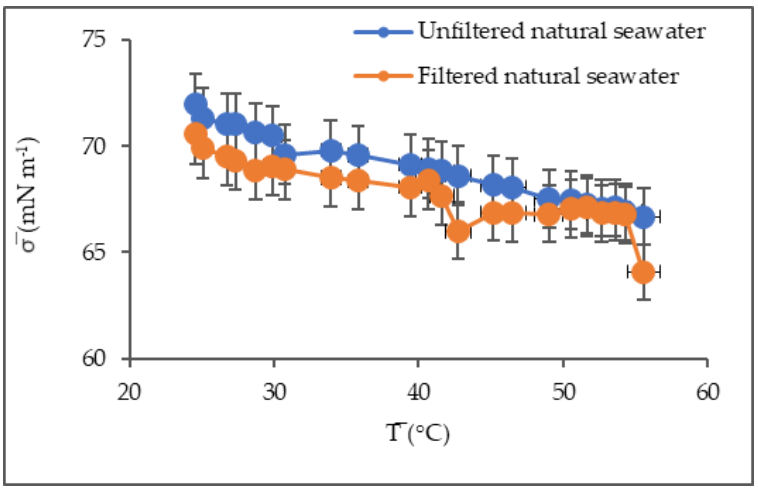

(**b**)

Figure 4. *Cont.*

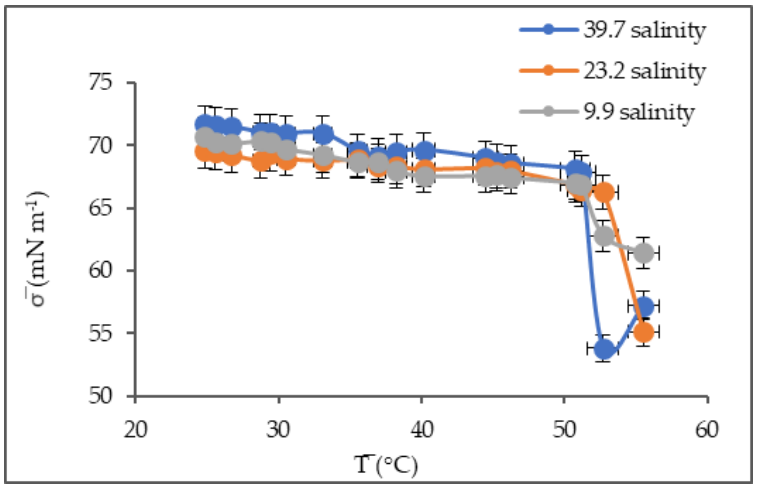

(**c**)

Figure 4. (**a**) Surface tension of deionized water as a function of temperature. (**b**,**c**) Temperature and salinity values in natural and artificial seawater. The surface tension of each sample decreased linearly with increased temperature.

3.4. Surface Tension of Deionized Water with Triton-X-100 and Oleyl Alcohol

In the first experiment, the surface tension of deionized water decreased very slowly and linearly with increasing Triton-X-100 concentrations at a temperature of 22 ± 2 °C. The decreasing surface tension continued until a concentration threshold was reached, at which point there was no further decrease, regardless of the further concentration of Triton-X-100 added (Figure 5a). Initially, the mean value of the measured surface tension of the deionized water sample was 71.8 ± 2 mN m^{-1}, which decreased to 71.0 ± 2 mN m^{-1} with Triton-X-100 at a concentration of 10.70 µg L^{-1}. The critical micelle concentration of Triton-X-100 in this study was observed to be 459 ± 59 µg L^{-1}.

In the second experiment (Figure 5b,c), 2000 µg L^{-1} of Triton-X-100 reduced the surface tension from 71.6 ± 2 mN m^{-1} to a mean of 39.4 ± 9 mN m^{-1}, which partially recovered to 57.6 mN m^{-1} within 30 min. The surface tension was constant for at least an additional 90 min thereafter. Oleyl alcohol decreased the surface tension similarly from 71.6 ± 2 to 38.7 ± 9 mN m^{-1} as soon as it was added to the deionized water samples. However, the surface tension did not recover and remained constant at 38.7 mN m^{-1} for the entire observation time of 120 min.

In a further experiment, the degree of recovery of the surface tension of deionized water was observed to be a function of the concentration of Triton-X-100 added to it with time. The surface tension decreased slowly with increasing concentrations but recovered within a few minutes. Initially, 13, 50, and 2000 µg L^{-1} of Triton-X-100 caused the surface tension levels to reduce from 71.6 ± 2 mN m^{-1} to 65.4 ± 3, 59.2, and 48.0 ± 1 mN m^{-1}, respectively, which then increased to 69.5 ± 2, 68.2 ± 1, and 60.4 ± 2 mN m^{-1}, respectively, after 5 min (Figure 5d). Further increases in surface tension was observed after 10 min of measurement. The surface tension levels of the deionized water samples treated with oleyl alcohol showed contrasting trends, as 13, 50, and 2000 µg L^{-1} of oleyl alcohol reduced the surface tension levels from 72.0 ± 1 mN m^{-1} to 53.8 ± 2, 44.0 ± 3, and 38.0 ± 6 mN m^{-1}, respectively, and these remained constant throughout the measurement periods (Figure 5e).

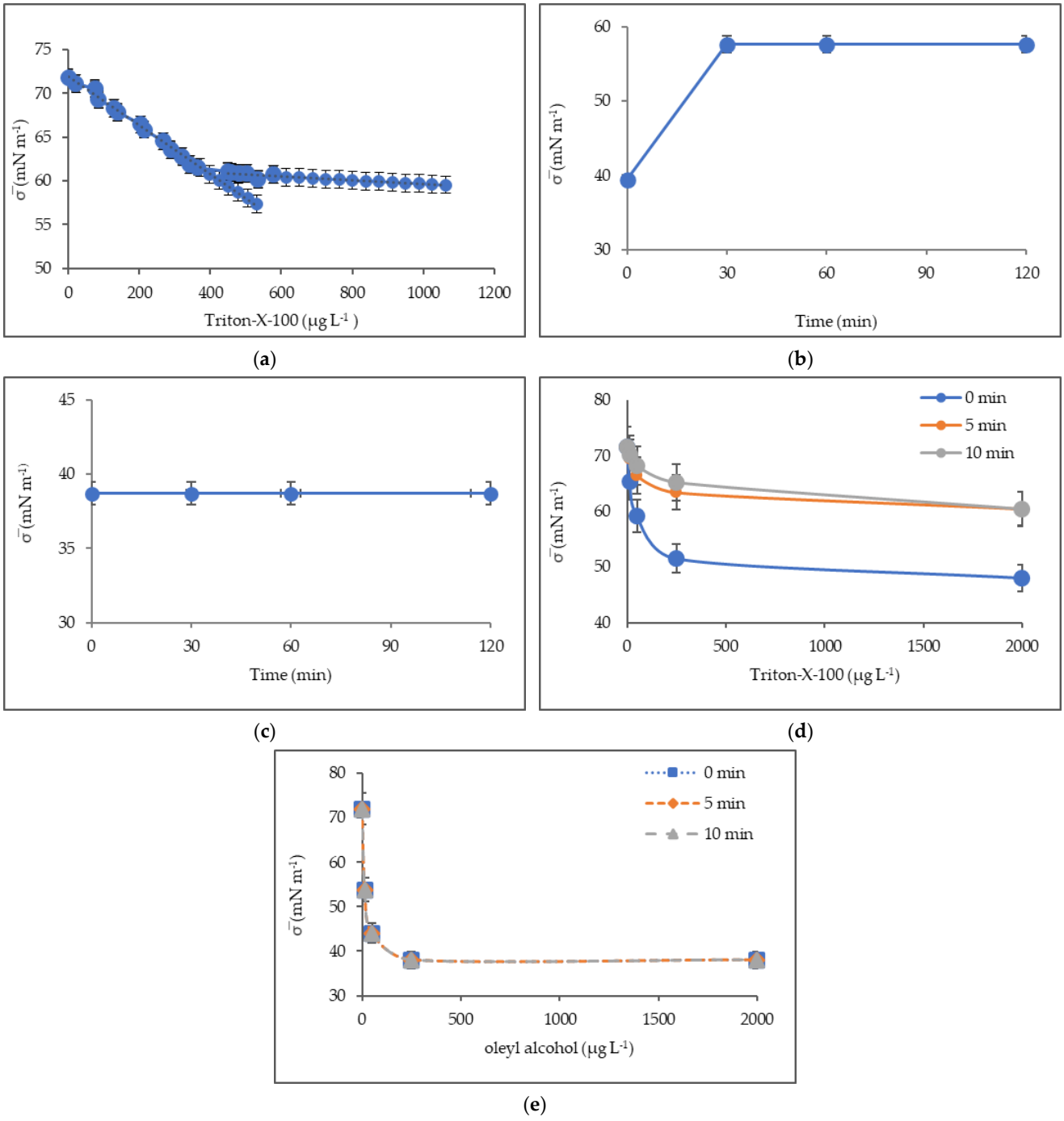

Figure 5. (**a**) Linear reduction in surface tension with varying concentrations of Triton-X-100. The critical average micelle concentration was 459 ± 59 µg L^{-1}. (**b**) Partial recovery of surface tension of deionized water was observed in treatment with Triton-X-100 within 30 min, which remained constant for the remaining 90 min. (**c**) Oleyl alcohol led to permanent suppression of the surface tension of deionized water for 120 min. (**d**) Surface tension of deionized water with Triton-X-100 was time-dependent; it partially recovered with time. (**e**) Surface tension of deionized water with oleyl alcohol was concentration-dependent; unlike with Triton-X-100, partial recovery was not observed.

4. Discussion

4.1. Oxygen Concentration, Exchange, and Suppression

We recorded different concentrations and observed consistent outfluxes of dissolved O_2 in the natural seawater and deionized water samples due to the nitrogen (i.e., O_2 free) head space in our experiments. With this approach, we forced significant outfluxes for

a mechanistic understanding of how natural SML and surfactants affect these outfluxes. While our measurements may have been affected by both filtration [24,25] and laboratory temperature [26] dissolved O_2 concentrations in seawater samples in all seasons were within the range specified by Parker et al. [27] and Romanescu et al. [28] in natural seawater. The saturation of our seawater samples with O_2 may, thus, have been linked to photosynthetic production, as discovered by Rahlff et al. [11].

O_2 was lost either through biological activities or molecular diffusion [6]. Although the exact process that led to biological utilization of O_2 was not assessed in this study, we cannot rule out additional losses through biological consumption [13,27,29]. Our samples from the semienclosed Jade Bay, with a strong tidal influence, had visually high concentrations of suspended particles, and bacterial respiration may have led to oxygen consumption [27,30].

On the other hand, enhanced photosynthetic activity was also apparent in our unfiltered natural seawater; we recorded higher dissolved O_2 concentrations in unfiltered than filtered seawater samples, regardless of the season they were collected. This indicates that phytoplankton and bacterial cells, as well as other organic materials suspended in unfiltered seawater, contribute to the production and consumption of dissolved O_2 [31]. However, Rahlff et al. [11] revealed that the O_2 concentration in seawater was produced mainly by the plankton, while only 7% was produced by the neuston. Although we collected our samples in different seasons and at different times and could corroborate our measurements in the laboratory with field measurements, we are aware that laboratory parameters may vary from in situ parameters. In situ parameters, including the dissolved O_2 concentration, salinity, and partial CO_2 pressure, are known to be significantly affected by the time of the day, phytoplankton exudates, and the season of the year [32].

Overall, the production and consumption of dissolved O_2 greatly influence the mineralization of particulate organic matter; Le Moigne et al. [31] reported a nearly 100% reduction in the degradation of particulate organic carbon and nitrogen in the absence of O_2. O_2 loss in filtered natural seawater was higher than that in unfiltered natural seawater; we recorded about 14% loss in the unfiltered samples collected in summer compared to about 31% in the filtered samples. As particulate material is an important component in SML formation, our observation stresses the importance of SML in reducing diffusion fluxes of O_2 across the water surface [33,34]. This was also supported by the fact that the addition of SML almost halted the loss of O_2 from the water to the nitrogen phase over a period of at least two hours.

Aside from the above, it is uncertain but possible that the reduced O_2 concentration in our samples from t_0 to t_{120} could be due to convective fluxes during evaporation and the movement of electrodes during our measurements. The thickness of the DBL points to convective fluxes, as the DBL was significantly larger than the values reportedly obtained from laboratory measurements [35]. Additionally, even though errors and sensor drifts were minimized by calibrating the microelectrode and temperature sensors before and after each experiment, Rahlff et al. [11] concluded that sensors can overestimate O_2 exchange from the upper water surface.

In general, natural and artificial sea surface films led to 78 and 81% reductions in O_2 diffusion across the surface of natural seawater and deionized water, respectively. This is not surprising, as Frew et al. [36] recorded ~5–50% suppression of O_2 diffusion caused by phytoplankton exudate, while Bock et al. [5] recorded ~90% reduction with artificial surfactants, including Triton-X-100. Furthermore, focusing on reduced CO_2 diffusion from the surfaces of seawater samples collected from the North Atlantic and Western Pacific Oceans, Ribas-Ribas et al. [13] and Mustaffa et al. [3] recently recorded about 54 and 62% reductions in CO_2 exchange, respectively, and defined a range of surfactant concentration in the SML of between 300 and 1000 $\mu g\ L^{-1}$. Since SMLs contain surface active agents of varying components and molecular weights, their role in the reduction in air–water gas exchange could be due to their role in changing the hydrodynamic behavior on the seawater surface, i.e., from a turbulent to a more laminar regime. The pressure force they

exert opposes turbulent eddy velocity, thereby interfering with energy transfer from the ocean surface [37].

Known to produce a damping effect on wave and turbulence intensity [38,39], the impediment of gas exchange produced by oleyl alcohol, also observed in our study, may create an artificial scenario not relevant for natural gas exchange processes. Oleyl alcohol has been used over the last four decades to mimic marine surface films [39], and even more recently to estimate the reduction in gas fluxes using artificial films in the North Atlantic [40]. The sea surface slick spread rapidly on the water surface, reacted very slowly with the water molecules, and then halted the movement of gas from the water surface into the air [41].

Unlike oleyl alcohol, Triton-X-100 is miscible with water, and from the observed reduction and partial recovery of surface tension of deionized water [6] at a concentration of 2000 μg L^{-1}, this is consistent with typical concentrations of surfactants between 800 and 2000 μg Teq L^{-1} observed in natural slicks [14]. As such, we suggest that Triton-X-100 resembles natural SML and reduces gas fluxes [19] without creating condensed monolayers, as oleyl alcohol.

4.2. Thickness of Diffusive Boundary Layer (DBL)

Our reported DBL thickness deviated from the ~60 μm attained by Zhengbin et al. [42] under natural conditions with microelectrodes, and also from the 50 ± 10 μm obtained by Zhengbin et al. [35] under both natural and laboratory conditions using various sampling methods. On a global scale, Broecker and Peng [43] estimated a thickness of 36 μm over the open ocean based on radon data, while Tsunogai and Noriyuki [34] estimated a range of 12 to 45 μm in situ. However, it has been experimentally shown that DBL thickness values obtained in the field vary considerably from those obtained under laboratory conditions [35,42].

The inclusion of higher surfactant concentrations on our stagnant water surfaces probably contributed to the relatively higher DBL thickness values obtained. This is not surprising, given that Rahlff et al. [11] deduced a thickness of 1100 μm from a stagnant seawater surface with a surfactant concentration of 2947 ± 3574 μg Teq L^{-1}. The immediate increased thickness of the DBL on deionized water treated with Triton-X-100 over time showed how rapidly the artificial film can spread on the water surface. It not only has the tendency to spread very fast even at low concentrations, but also the ability to be homogenized and maintain its thin film structure within the sublayer for several hours [9].

The DBL in the unfiltered natural seawater was thicker than that of filtered seawater, which was expected because filtration partly removes surface-active agents by adsorption on filter surfaces [44]. Additionally, enrichment factors and higher abundances of cells probably contribute to the character of the SML as a DBL. Enrichment factors and bacterial biomass were observed by Wurl et al. [22] to be an order of magnitude higher in the SML than in the underlying seawater in the North Pacific Ocean and South China and Baltic Seas. We observed variability in both the replicate measurements at each time point and the pooled thicknesses over a course of 120 min in our deionized water samples. However, the variability of the DBL thickness in natural seawater (filtered and unfiltered) with SML was greater than in the deionized water with monolayers of Triton-X-100 and oleyl alcohol due to the complex and dynamic composition of natural seawater. This means that even though the surfactants present in SML are known to effect air–water gas flux [3,13], they differ considerably in their chemical composition [45], which with the absolute concentrations of surfactants, determines the extent of reduction in the air–water gas flux.

The residence time of surfactants in the DBL can vary depending on the chemical nature, because the interactions between the different molecules in the SML create thick, highly complex layers rather than well-organized layers. For example, more recent study confirmed a seminal hypothesis [46] that under certain conditions, natural SML may develop biofilm-like properties with a much thicker DBL, similar to laboratory studies [11].

Our DBL measurements revealed a constant thickness in deionized water without any additional treatment over a period of 120 min (see Section 3.2). Even though the water was obtained from a laboratory-based ultrapure system, pure water may not be 100% pure, as small quantities of dissolved organic matter remains in purified water [15]. Wurl and Sin [47] assessed the levels of organic material in deionized water from different sources and found that the water contained on average 10 µmol C/L of dissolved organic matter. Additionally, the formation and maintenance of organic-free water surfaces is not possible due to cross-contamination from the materials used for measurement (beaker and immersed micro profiler) as well as the overlying air [45]. Even with thorough cleaning, it is impossible to have these materials totally free of organic matter, and in particular surfactants can stick tenaciously to their surfaces. Handling and exposure to the laboratory air will also add additional materials.

Overall, a level of 60–80 µmol C/L, similar to oligotrophic ocean water, in our deionized water may have occurred, leading to the formation of a microlayer, as observed in the most remote regions of the ocean. The thick layer obtained from our deionized water samples may also have originated from the thermal boundary layer, i.e., a cooler temperature at the air–water interface due to the loss of evaporative heat [8,13], as we did not attempt to minimize evaporative fluxes. This means that the DBL reported here could represent the combined effects of thermal and mass diffusion [48].

In reference to our measurements in deionized water, the DBL formed by Triton-X-100 was insignificantly thicker than that formed by oleyl alcohol, which can be explained by the relatively high concentration of 2000 µg L^{-1}, which was well above the 449 and 50 µg L^{-1} (Figures 3a and 4e) for the estimated micelle concentrations of Triton X-100 and oleyl alcohol, respectively. This means that any excess molecules remaining after the formation of a monolayer produced micelles in the bulk water, and as we added each surfactant gently to the stagnant water surface, micelles were probably formed very near the air–water interface, which in turn contributed to the formation of the relatively thick DBL compared to SML. However, we chose the concentration of 2000 µg L^{-1} to resemble typical concentration ranges for natural slicks [14]. This can also be assumed to be the reason why the two surfactants reduced gas exchange between the water and the air, because the higher the DBL, the lower the probability of gaseous molecules travelling in the air, and hence the lower the concentration loss.

4.3. Surface Tension

Our surface tension values for deionized water ranged from 71.82 to 72.00 mN m^{-1} at 24 ± 1 °C, which diverged from the 72.62 mN m^{-1} at 20 °C reported by Richard and Coombs [49] and 72.25 mN m^{-1} at 20 °C reported by Harkins and Young [50]. The deviation was probably due to differences in the temperature at which the measurements were taken. The linearity relationship with temperature agrees with those compiled and obtained by Vargaftik et al. [51] and Schmidt and Schneider [19]. Jian et al. [52] calculated the numbers of hydrogen bonds formed by water molecules at different temperatures and observed a decrease in hydrogen bonds per water molecule with increasing temperature. This explains the lower surface tension with increasing temperature observed in our study, and the same effect may occur in natural seawater.

The surface tension of natural and artificial seawater increase with salinity because salt concentrations increase the surface tension of water [53]. However, Schmidt and Schneider [19] observed a higher surface tension (~73 mN m^{-1} at 25 °C and salinity of 11.5) for natural seawater obtained from the Baltic Sea compared to pure water. Nayar et al. [18], on the other hand, observed that the surface tension of artificial seawater was ~73 mN m^{-1} at a temperature of ~20 °C and salinity of 20. Wang et al. [54] measured a surface tension of ~76 mN m^{-1} for both deionized water and 3.5 wt% NaCl solution. Molecularly, sodium and chloride ions hydrate in water and orientate themselves on the surface by aligning with the water molecules to form a strong cohesive force, thereby increasing the amount

of work that needs to be done to create a unit area on the water surface, leading to higher surface tension [45].

Although the surface tension of our deionized water sample was higher than that of natural and artificial seawater at the same temperature, making this study fall in line with other studies, the surface tension values were not as high as those previously reported, and this could be due to the following reasons. For example, in their study, Schmidt and Schneider [19] worked with low-surfactant seawater samples, while Nayar et al. [18] worked with artificial seawater samples completely devoid of any surface-active materials. Thus, while the natural seawater samples in our study were only filtered through 0.22 µm membranes, other studies rigorously removed all surface-active substances by solid phase extraction, which renders seawater nearly free from all polar and aromatic compounds without affecting the salinity. Even though filtration removes a fraction of dissolved surfactants by adsorption on the filter surfaces [44], conventional filtration is insufficient to efficiently remove surfactants. Depending on the concentration, the presence of surfactant lowers the surface tension, and therefore compensates or completely masks the increase in surface tension by the presence of salt ions [55].

The sharp decrease between 51 and 52 °C observed in two of the three artificial seawater samples probably occurred because the surface tension depends on hydrogen bonds, although with increasing temperature, the water molecules move or vibrate quicker. This may have caused instability of the surface tension of our artificial seawater, and it seems 50 °C is a threshold at which the surface tension loses much of its strength.

We recorded reductions in surface tension (in reference to pure water) with Triton X-100 and oleyl alcohol at concentrations between 13 and 2000 µg L^{-1}. The magnitude of reduction increased with increasing concentration. As previously stated, Triton-X-100 behaved more similarly to natural slicks than oleyl alcohol did. The concentrations of surfactant in natural SML vary between tens to thousands of µg Teq L^{-1} i.e., equivalent to Triton X-100. Therefore, lower concentrations of Triton-X-100 (13–200 µg Teq L^{-1}) can reduce the surface tension by 5 mN m^{-1} (Figure 5a), similar to an earlier study [18]. Above a concentration of 200 µg Teq L^{-1}, the air–water CO_2 transfer velocity is reduced by 23 and 32% based on field studies [3,56], and we observed a continuing reduction in surface tension by 16 mN m^{-1} for concentrations equivalent to slick conditions, i.e., above 800 µg Teq L^{-1}. In addition, our results show that the application of Triton-X-100 in the air–water gas exchange process requires care in terms of its dynamic behavior in regulating surface tension (Figure 5d).

Unlike Triton-X-100, treatment with 13 to 2000 µg L^{-1} of oleyl alcohol resulted in a sharp decrease in the surface tension of deionized water, which remained static for the entire period of measurement (Figure 5e). This explains the tendency of the surfactant to remain stable and retain its polymerized structure at the water–air interface [9]. Due to its capability to form condensed films at low concentrations, we suggest that oleyl alcohol does not resemble natural SML well but represents the behavior of slicks. Slicks cover no more than 10% of the open ocean [24]; therefore, laboratory and field studies utilizing oleyl alcohol as an artificial film are probably not mimicking the typical air–water gas exchange process over the open ocean.

5. Conclusions

Our study revealed variations in oxygen concentrations and the impact of surfactants on the thickness of the diffusive boundary layer. We showed that natural SML and condensed artificial films reduced the evasion of oxygen, and from our results we concluded that increasing concentrations of surfactants increased the thickness of the DBL with further reductions in air–gas fluxes. The DBL thickening effect was more prominent with artificial surfactants and not for natural SMLs. Future studies utilizing artificial films should consider our observations. Our determined micelle concentrations for Triton-X-100 and oleyl alcohol were within typical ranges of natural surfactants in the SML. Future studies are needed to confirm the presence and concentration of micelles, as they may

control the fate of hydrophobic organic matter on the ocean surface. The partial recovery of the surface tension of deionized water observed with Triton-x100 disappeared by the end of the measuring period, further stressing the ability of Triton-X-100 to act as a natural slick even at low concentrations. The concentrations of Triton-X-100 and oleyl alcohol presented in this study represent the threshold of natural slicks, and from our results we concluded that artificial films made of Triton X-100 represent the behavior of natural SMLs, whereas oleyl alcohol forms condensed films typical of marine slicks. We acknowledge that complementary laboratory and field studies are a challenge for ocean science, although both approaches are needed for a mechanistic understanding of the future ocean. Our study is important because of its usefulness in providing an understanding of the impacts of surfactants on the dynamics of important processes occurring across the sea surface microlayer.

Author Contributions: Conceptualization, M.R.-R. and O.W.; methodology, A.A. and M.H.; writing—original draft preparation A.A. and O.W.; writing—review and editing A.A., M.R.-R., O.W. and C.S.; supervision, M.R.-R. and O.W.; funding acquisition, O.W. All authors have read and agreed to the published version of the manuscript.

Funding: This research was funded by the European Research Council (ERC), grant number GA336408. During the writing process M.R.-R. was funded by Deutsche Forschungsgemeinschaft (DFG, German Research Foundation)—Project number 427614800 and A.A. was funded by Katholischer Akademischer Ausländer-Dienst: KAAD.

Data Availability Statement: https://doi.org/10.1594/PANGAEA.937780 (accessed on 10 November 2021).

Acknowledgments: We thank Bernd Schneider (institute for Baltic Sea Research Warnemünde) for the loan of a tensiometer. We also want to thank Carola Lehners for her technical support during the surface tension measurements.

Conflicts of Interest: The authors declare no conflict of interest.

References

1. Wurl, O.; Ekau, W.; Landing, W.M.; Zappa, C.J.; Bowman, J. Sea surface microlayer in a changing ocean—A perspective. *Elem. Sci. Anthr.* **2017**, *5*, 31. [CrossRef]
2. Schimpf, U.; Garbe, C.; Jähne, B. Investigation of transport processes across the sea surface microlayer by infrared imagery. *J. Geophys. Res. Ocean.* **2004**, *109*, C08S13. [CrossRef]
3. Mustaffa, N.I.H.; Ribas-Ribas, M.; Banko-Kubis, H.M.; Wurl, O. Global reduction of in situ CO_2 transfer velocity by natural surfactants in the sea-surface microlayer. *Proc. R. Soc. A* **2020**, *476*, 20190763. [CrossRef]
4. Garbe, C.S.; Rutgersson, A.; Boutin, J.; De Leeuw, G.; Delille, B.; Fairall, C.W.; Gruber, N.; Hare, J.; Ho, D.T.; Johnson, M.T.; et al. Transfer across the air-water interface. In *Ocean-Atmosphere Interactions of Gases and Particles*; Springer: Berlin/Heidelberg, Germany, 2014; pp. 55–112.
5. Bock, E.J.; Hara, T.; Frew, N.M.; McGillis, W.R. Relationship between air-sea gas transfer and short wind waves. *J. Geophys. Res. Ocean.* **1999**, *104*, 25821–25831. [CrossRef]
6. Zappa, C.J.; Raymond, P.A.; Terray, E.A.; McGillis, W.R. Variation in surface turbulence and the gas transfer velocity over a tidal cycle in a macro-tidal estuary. *Estuaries* **2003**, *26*, 1401–1415. [CrossRef]
7. Jahne, B.; Münnich, K.O.; Siegenthaler, U. Measurements of gas exchange and momentum transfer in a circular wind-water tunnel. *Tellus* **1979**, *31*, 321–329. [CrossRef]
8. Schrage, R.W. *A Theoretical Study of Interphase Mass Transfer*; Columbia University Press: New York, NY, USA, 1953.
9. Mallinger, W.D.; Mickelson, T.P. Experiments with monomolecular films on the surface of the open sea. *J. Phys. Oceanogr.* **1973**, *3*, 328–336. [CrossRef]
10. Gundersen, J.K.; Jorgensen, B.B. Microstructure of diffusive boundary layers and the oxygen uptake of the sea floor. *Nature* **1990**, *345*, 604–607. [CrossRef]
11. Rahlff, J.; Stolle, C.; Giebel, H.A.; Ribas-Ribas, M.; Damgaard, L.R.; Wurl, O. Oxygen profiles across the sea-surface microlayer—Effects of diffusion and biological activity. *Front. Mar. Sci.* **2019**, *6*, 11. [CrossRef]
12. Revsbech, N.P.; Madsen, B.; Jørgensen, B.B. Oxygen production and consumption in sediments determined at high spatial resolution by computer simulation of oxygen microelectrode data. *Limnol. Oceanogr.* **1986**, *31*, 293–304. [CrossRef]
13. Ribas-Ribas, M.; Helleis, F.; Rahlff, J.; Wurl, O. Air-water CO2-exchange in a large annular wind-wave tank and the effects of surfactants. *Front. Mar. Sci.* **2018**, *5*, 457. [CrossRef]
14. Wurl, O.; Miller, L.; Röttgers, R.; Vagle, S. The distribution and fate of surface-active substances in the sea-surface microlayer and water column. *Mar. Chem.* **2009**, *115*, 1–9. [CrossRef]

15. Jarvis, N.L.; Garrett, W.D.; Scheiman, M.A.; Timmons, C.O. Surface chemical characterization of surface-active material in seawater. *Limnol. Oceanogr.* **1967**, *12*, 88–96. [CrossRef]
16. Serafini, P.; Leyes, M.F.; Pereyra, R.B.; Schulz, E.P.; Durand, G.A.; Schulz, P.C.; Ritacco, H.A. The aqueous Triton X-100–dodecyltrimethylammonium bromidemicellar mixed system. Experimental results and thermodynamic analysis. *Colloids Surf. A Physicochem. Eng. Asp.* **2018**, *559*, 127–135. [CrossRef]
17. Knepper, T.P.; de Voogt, P.; Barcelo, D. *Analysis and Fate of Surfactants in the Aquatic Environment*; Elsevier: Amsterdam, The Netherlands, 2003.
18. Nayar, K.G.; Panchanathan, D.; McKinley, G.H.; Lienhard, J.H. Surface tension of seawater. *J. Phys. Chem. Ref. Data* **2014**, *43*, 043103. [CrossRef]
19. Schmidt, R.; Schneider, B. The effect of surface films on the air–sea gas exchange in the Baltic Sea. *Mar. Chem.* **2011**, *126*, 56–62. [CrossRef]
20. Schückel, U.; Beck, M.; Kröncke, I. Spatial variability in structural and functional aspects of macrofauna communities and their environmental parameters in the Jade Bay (Wadden Sea Lower Saxony, southern North Sea). *Helgol. Mar. Res.* **2013**, *67*, 121–136. [CrossRef]
21. Harvey, G.W.; Burzell, L.A. A simple microlayer method for small samples 1. *Limnol. Oceanogr.* **1972**, *17*, 156–157. [CrossRef]
22. Wurl, O.; Stolle, C.; Van Thuoc, C.; Thu, P.T.; Mari, X. Biofilm-like properties of the sea surface and predicted effects on air–sea CO2 exchange. *Prog. Oceanogr.* **2016**, *144*, 15–24. [CrossRef]
23. Romano, J.C. Sea-surface slick occurrence in the open sea (Mediterranean, Red Sea, Indian Ocean) in relation to wind speed. *Deep. Sea Res. Part I Oceanogr. Res. Pap.* **1996**, *43*, 411–423. [CrossRef]
24. Petters, S.S.; Petters, M.D. Surfactant effect on cloud condensation nuclei for two-component internally mixed aerosols. *J. Geophys. Res. Atmos.* **2016**, *121*, 1878–1895. [CrossRef]
25. Saunders, P.M. The accuracy of measurement of salinity, oxygen and temperature in the deep ocean. *J. Phys. Oceanogr.* **1986**, *16*, 189–195. [CrossRef]
26. Gallaher, W.U. Dissolved Oxygen Changes During Filtration. *J. Am. Water Work. Assoc.* **1927**, *17*, 476–480. [CrossRef]
27. Parker, C.A.; O'Reilly, J.E. Oxygen depletion in Long Island Sound: A historical perspective. *Estuaries* **1991**, *14*, 248–264. [CrossRef]
28. Romanescu, G.; Stoleriu, C.C. Seasonal Variation of Temperature, p H, and Dissolved Oxygen Concentration in Lake Rosu, Romania. *CLEAN–Soil Air Water* **2014**, *42*, 236–242. [CrossRef]
29. Sieburth, J.M. *Microbiological and Organic-Chemical Processes in the Surface and Mixed Layers in Air-Sea Exchange of Gases and Particles 1983*; Springer: Dordrecht, The Netherlands; pp. 121–172.
30. Obernosterer, I.; Catala, P.; Reinthaler, T.; Herndl, G.J.; Lebaron, P. Enhanced heterotrophic activity in the surface microlayer of the Mediterranean Sea. *Aquat. Microb. Ecol.* **2005**, *39*, 293–302. [CrossRef]
31. Le Moigne, F.A.; Cisternas-Novoa, C.; Piontek, J.; Maßmig, M.; Engel, A. On the effect of low oxygen concentrations on bacterial degradation of sinking particles. *Sci. Rep.* **2017**, *7*, 1–12. [CrossRef] [PubMed]
32. Yates, K.K.; Dufore, C.; Smiley, N.; Jackson, C.; Halley, R.B. Diurnal variation of oxygen and carbonate system parameters in Tampa Bay and Florida Bay. *Mar. Chem.* **2007**, *104*, 110–124. [CrossRef]
33. Goldman, J.C.; Dennett, M.R.; Frew, N.M. Surfactant effects on air-water gas exchange under turbulent conditions. *Deep. Sea Res. Part A Oceanogr. Res. Pap.* **1988**, *35*, 1953–1970. [CrossRef]
34. Tsunogai, S.; Tanaka, N. Flux of oxygen across the air-sea interface as determined by the analysis of dissolved components in sea water. *Geochem. J.* **1980**, *14*, 227–234. [CrossRef]
35. Zhengbin, Z.; Liansheng, L.; Zhijian, W.; Jun, L.; Haibing, D. Physicochemical studies of the sea surface microlayer: I. Thickness of the sea surface microlayer and its experimental determination. *J. Colloid Interface Sci.* **1998**, *204*, 294–299. [CrossRef] [PubMed]
36. Frew, N.M.; Goldman, J.C.; Dennett, M.R.; Johnson, A.S. Impact of phytoplankton-generated surfactants on air-sea gas exchange. *J. Geophys. Res. Ocean.* **1990**, *95*, 3337–3352. [CrossRef]
37. Carpenter, L.J.; Archer, S.D.; Beale, R. Ocean-atmosphere trace gas exchange. *Chem. Soc. Rev.* **2012**, *41*, 6473–6506. [CrossRef] [PubMed]
38. Broecker, H.C.; Petermann, J.; Siems, W. The influence of wind on CO_2-exchange in a wind-wave tunnel, including the effects of monolayers. *J. Mar. Res.* **1978**, *36*, 595–610.
39. Brockmann, U.H.; Huhnerfuss, H.; Kattner, G.; Broecker, H.C.; Hentzschel, G. Artificial surface films in the sea area near Sylt 1. *Limnol. Oceanogr.* **1982**, *27*, 1050–1058. [CrossRef]
40. Salter, M.E.; Upstill-Goddard, R.C.; Nightingale, P.D.; Archer, S.D.; Blomquist, B.; Ho, D.T.; Huebert, B.; Schlosser, P.; Yang, M. Impact of an artificial surfactant release on air-sea gas fluxes during Deep Ocean Gas Exchange Experiment II. *J. Geophys. Res. Ocean.* **2011**, *116*, C11016. [CrossRef]
41. Barger, W.R.; Garrett, W.D.; Mollo-Christensen, E.L.; Ruggles, K.W. Effects of an artificial sea slick upon the atmosphere and the ocean. *J. Appl. Meteorol.* **1970**, *9*, 396–400. [CrossRef]
42. Zhang, Z.; Cai, W.; Liu, L.; Liu, C.; Chen, F. Direct determination of thickness of sea surface microlayer using a pH microelectrode at original location. *Sci. China Ser. B Chem.* **2003**, *46*, 339–351. [CrossRef]
43. Peng, T.H.; Broecker, W.S.; Mathieu, G.G.; Li, Y.H.; Bainbridge, A.E. Radon evasion rates in the Atlantic and Pacific Oceans as determined during the GEOSECS program. *J. Geophys. Res. Ocean.* **1979**, *84*, 2471–2486. [CrossRef]
44. Dragcevic, D.; Vukovic, M.; Cukman, D.; Pravdic, V. Properties of the seawater-air interface. Dynamic surface tension studies 1. *Limnol. Oceanogr.* **1979**, *24*, 1022–1030. [CrossRef]
45. Frew, N.M.; Nelson, R.K. Scaling of marine microlayer film surface pressure-area isotherms using chemical attributes. *J. Geophys. Res. Ocean.* **1992**, *97*, 5291–5530. [CrossRef]

46. Zhang, X.; Han, J.; Zhang, X.; Shen, J.; Chen, Z.; Chu, W.; Kang, J.; Zhao, S.; Zhou, Y. Application of Fourier transform ion cyclotron resonance mass spectrometry to characterize natural organic matter. *Chemosphere* **2020**, *260*, 127458. [CrossRef] [PubMed]
47. Wurl, O.; Sin, T.M. Analysis of dissolved and particulate organic carbon with the HTCO technique. In *Practical Guidelines for the Analysis of Seawater*; CRC Press: Boca Raton, FL, USA, 2009; pp. 45–60.
48. Gebhart, B.; Pera, L. The nature of vertical natural convection flows resulting from the combined buoyancy effects of thermal and mass diffusion. *Int. J. Heat Mass Transf.* **1971**, *14*, 2025–2050. [CrossRef]
49. Richards, T.W.; Coombs, L.B. The surface tensions of water, methyl, ethyl and isobutyl alcohols, ethyl butyrate, benzene and toluene. *J. Am. Chem. Soc.* **1915**, *37*, 1656–1676. [CrossRef]
50. Harkins, W.D.; Young, T.F.; Cheng, L.H. The ring method for the determination of surface tension. *Science* **1926**, *64*, 333–336. [CrossRef]
51. Vargaftik, N.B.; Volkov, B.N.; Voljak, L.D. International tables of the surface tension of water. *J. Phys. Chem. Ref. Data* **1983**, *12*, 817–820. [CrossRef]
52. Jian, C.; Poopari, M.R.; Liu, Q.; Zerpa, N.; Zeng, H.; Tang, T. Mechanistic understanding of the effect of temperature and salinity on the water/toluene interfacial tension. *Energy Fuels* **2016**, *30*, 10228–10235. [CrossRef]
53. Sghaier, N.; Prat, M.; Nasrallah, S.B. On the influence of sodium chloride concentration on equilibrium contact angle. *Chem. Eng. J.* **2006**, *122*, 47–53. [CrossRef]
54. Wang, X.; Chen, C.; Poeschl, U.; Su, H.; Cheng, Y. Molecular Dynamics Simulation of Surface Tension of NaCl Aqueous Solution at 298.15 K: From Diluted to Highly Supersaturated Concentrations. *EGUGA* **2017**, *19*, 1015.
55. Zhang, C.; Carloni, P. Salt effects on water/hydrophobic liquid interfaces: A molecular dynamics study. *J. Phys. Condens. Matter* **2012**, *24*, 124109. [CrossRef]
56. Pereira, R.; Ashton, I.; Sabbaghzadeh, B.; Shutler, J.D.; Upstill-Goddard, R.C. Reduced air–sea CO_2 exchange in the Atlantic Ocean due to biological surfactants. *Nat. Geosci.* **2018**, *11*, 492–496. [CrossRef]